3D field analysis in 3-phase amorphous modular transformer under increased frequency operation

BRONISŁAW TOMCZUK, DARIUSZ KOTERAS

Opole University of Technology, Department of Industrial Electrical Engineering
ul. Prószkowska 76, 45-758 Opole
e-mail: b.tomczuk@po.opole.pl, d.koteras@po.opole.pl

Abstract: The calculations results of the temperature distribution in a 3-phase transformer with modular amorphous core are presented. They were performed for two frequency values which were higher than the power system one. For the 3D field analyses the Finite Element Method (FEM) was used. The calculated temperature at the points of the core surface has been verified using an infrared camera.

Key words: 3D field analysis, temperature calculation, eddy current losses, measurement tests

1. Introduction

The 3-phase and one-phase transformers are widely used in many appliances. In a lot of electrical devices they are operating under with higher frequency than that which is supplying the power system. The eddy current losses in their magnetic cores depend strongly on the supplying frequency. Thus, the modern magnetic circuits of the transformers are manufactured using amorphous ribbon, which characterises much lower core losses than the grain oriented silicon steel [6]. Its thickness is about 30 μm, thus it is nearly impossible to analyze the 3D magnetic field in each separate thin core scroll or in each amorphous thin sheet.

Calculations of the eddy currents or hysteresis losses in laminated cores are quite difficult [10], especially for the amorphous transformers [4-6]. Thus, in the 3D analysis all designers assume the magnetic core as a solid region. However it is difficult to determine the equivalent parameters for such a solid core. In this work we have determined those parameters and calculated the eddy current losses values in the amorphous magnetic core, and the results have been compared with the measured ones.

2. Physical object and its numerical model

2.1. Geometry of the transformer

In our work, the 3-phase transformer with amorphous modular core has been investigated. The rated power of the transformer, under $f = 50$ Hz frequency supplying, is equal to $S = 10$ kVA.

The assumed coordinate system and main dimensions (in mm) of the transformer geometry are presented in Figure 1. The supplied coils which are divided into two sections, had $N = 116$ turns. The first section is wounded with $N_1 = 20$ turns and the second one has $N_2 = 96$ turns.
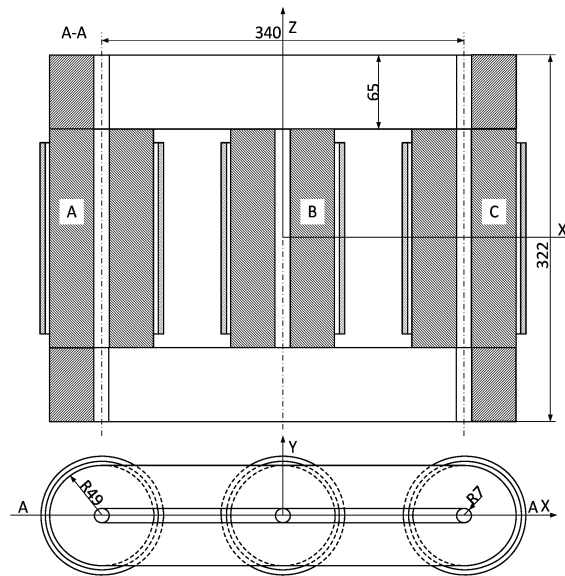

Fig. 1. Main dimensions of the analysed transformer

2.2. Numerical model

For the magnetic and thermal field analysis the Finite Element Method has been applied. Due to the symmetry of the analysed object, the numerical models have included only half geometry of the transformer.

In the regions where the eddy currents arise, the partial differential equations for the total vector potential $\vec{A}$ and the electric scalar potential V have to be satisfied

$$\nabla \times \frac{1}{\mu} \nabla \times \vec{A} = -\sigma \frac{\partial \vec{A}}{\partial t} - \sigma \nabla V, \tag{1}$$

$$\nabla \cdot \sigma \nabla V + \nabla \cdot \sigma \frac{\partial \vec{A}}{\partial t} = 0, \tag{2}$$

where: σ – electrical conductivity, μ – magnetic permeability of the material.

The module Elektra SS from Opera 3D package has been employed for the eddy current distribution in the core. The algorithm of that module are based on the combination of total ($\vec{A}_T$) and reduced ($\vec{A}_R$) vector potentials for modelling the time varying electromagnetic fields [1]. As the coils are wounded with wire of small cross section, the eddy current losses in the coils can be neglected. However, the Joule losses in the coils have been taken into account, naturally.

The thermal field in the transformer geometry has been analysed using the Opera-3D/Tempo solver [3]. For the thermal static calculations, Poisson equation (Eq. 3) has been solved [2, 8] to determine the temperature (T) distribution

$$\nabla \cdot (\kappa \nabla T) = -Q,$$
(3)

where: κ – thermal conductivity [W/(m · K)], Q – feed thermal power density [W/m^3].

To execute the thermal transient simulations, the parabolic-elliptic partial differential equation should be formulated and solved

$$\rho \, c \frac{\partial T}{\partial t} - \nabla \cdot (\kappa \nabla T) = Q,$$
(5)

where: ρ – mass density [kg/m^3], c – thermal capacitance [J/(kg · K)] κ – thermal conductivity [W/(m · K)], Q – feed thermal power density [W/m^3].

Dirichlet's conditions for the temperature have been assumed on the calculation region boundaries. The ambient temperature (T_0 = 25ºC) has been applied at the edges of the calculated region. On the surface of the transformer solid, the convection and radiation phenomena has been adopted. The equivalent radiation coefficient h_{eq} ([7]) has been calculated with the expression (Eq. 5)

$$h_{eq} = h + 4\sigma_B \varepsilon ((T + T_0)/2)^3,$$
(5)

where: σ_B – Stefan-Boltzmann constant ($5,67 \cdot 10^{-8}$ [W/(m^{2}K^4)]), ε – the emittance value.

For the coil heating determination, the Ohmic losses density values were calculated with the well-known relation

$$Q = (RI^2)/V_{coil},$$
(6)

where: R – winding resistance [Ω], I – rms value of the current intensity [A], V_{coil} – volume of the winding [m^3].

3. Calculation results and measured verification

We analyzed the transformer which has been supplied with sinusoidal current under two frequencies f_1 = 500 Hz and f_2 = 250 Hz. The number of the turns coil in each phase was equal to N_1 = 20. The assumed amplitudes of the currents for the phases *A* and *C* were equal to $I_{Am} = I_{Cm}$ = 3.64 A, and for the phase *B* the amplitude I_{Bm} was equal to 3.22 A. Due to low values of the average magnetic flux density inside the magnetic circuit, the two different values of the relative magnetic permeability μr have been adopted. For the yoke region the value μ_r = 20713 has been assumed. As the magnetic flux in each column is perpendicular to ribbon rolling, the relatively small value of permeability has taken (μ_r = 2067).

The amorphous cores are built as the laminated structures. The thickness of the lamination ribbon is approximately equal to 30 μm. Due to difficulty in the modelling of each tape layer independently each to other, the 3D eddy current problems should be solved using a solid geometry of the core. Thus, the equivalent electrical conductivity of the core should be determined. Lately, it was introduced the technique for the calculation of the equivalent conduc-

tivity for a stack of silicon steel sheets [9]. However, the approach is not useful for the amorphous laminated magnetic circuits. Thus, we determined the equivalent conductivity from the tests of the physical model, and iterative calculation. For the field analyses the equivalent conductivity was assumed σ_{eq} = 450 S/m. Under frequency of f_1 = 500 Hz the total core losses are equal to P_{Fe}=270 W. Although the amorphous material conductivity is equal to σ = 0,769 · 10^6 S/m, the equivalent one for the homogenized solid core, for the magnetic field analysis should be significantly lower.

It is almost impossible the field modeling in the actual amorphous lamination structure. For the 3D numerical analyses of the calculated magnetic cores we substitute a real laminated core for the solid one of the same exterior dimensions. Thus, we need to replace the real magnetic circuit by the solid geometry with equivalent parameters (magnetic permeability, electrical conductivity). In our paper the assumed equivalent conductivity was calculated using below relation

$$\sigma_{eq} = \frac{1}{k_{Fe}} \left(\frac{d}{b} \right)^{0,89} \cdot \sigma_{Am}, \tag{7}$$

where: d – thickness of the amorphous ribbon, b – average length of the amorphous ribbon in leg, σ_{Am} – electrical conductivity of the amorphous tape material.
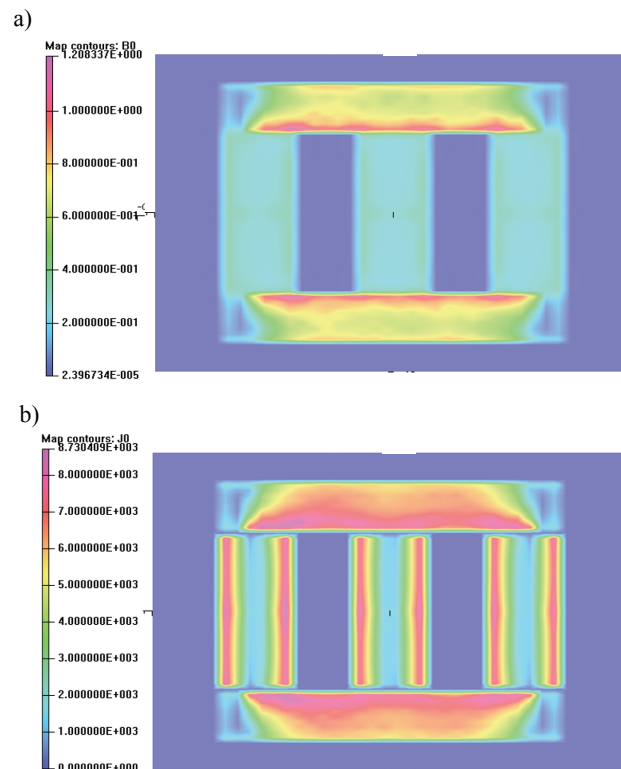
a)

b)

Fig. 2. Field distributions on the surface XZ_1, f_1 = 500 Hz a) magnetic flux density,
b) eddy current density

In Figures 2 and 3 we presented the distributions of the magnetic flux and the eddy currents densities at the points of the surface XZ_1 which is parallel to the XZ plane (Fig. 1). The surface is shifted by 1 cm from the XZ plane. Figures 2a and 2b concern the frequency value $f_1 = 500$ Hz. In Figures 3a and 3b we presented the magnetic flux and eddy current distributions which have been obtained under frequency supplying of $f_2 = 250$ Hz.
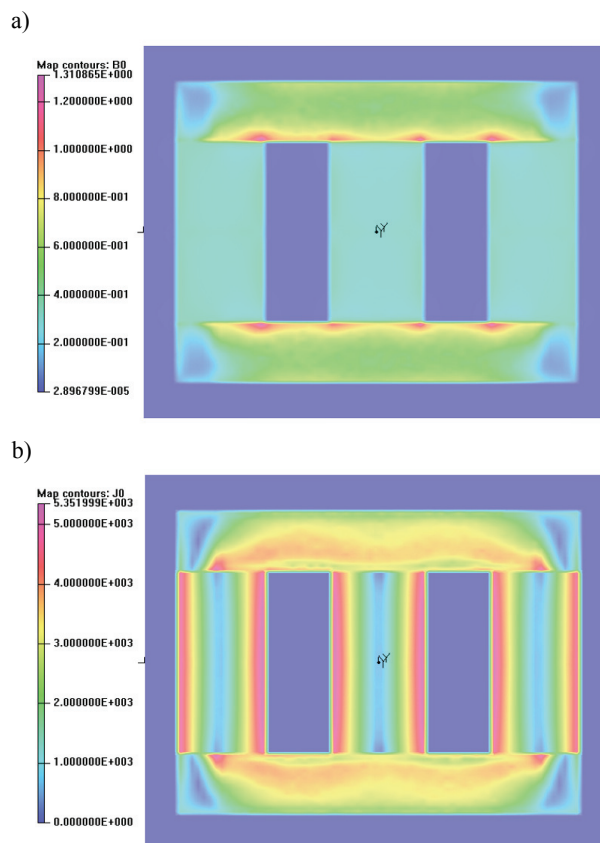
a)

b)

Fig. 3. Field distributions on the surface XZ_1, $f_2 = 250$ Hz: a) magnetic flux density,
b) eddy current density

The adequate fields presented in Figures 2 and 3 are similar in distributions for both analysed frequencies. Due to the assumed low value of the electrical conductivity ($\sigma_{eq} = 450$ S/m) to the numerical model nearly the same level of the magnetic flux density B inside of transformer legs, have been obtained. In the yokes of the object the maximal values of the B are occurred near the transformer windows. For the frequency $f_2 = 250$ Hz the maximal values are slightly higher than those frequency $f_1 = 500$ Hz.

The eddy current densities for the two frequencies ($f_1 = 500$ Hz, $f_2 = 250$ Hz) a quite different each from other, naturally. For the frequency f_1, the maximal values are lower than $J = 9$ kA/m², while for the twice lower frequency the maximal value is approximately $J = 5.4$ kA/m².

Field analyses

The obtained spatial distributions of the eddy current losses inside the magnetic core has been taken as the input data for the thermal model. In Figures 4 and 5, the static thermal field distributions in the 3-phase transformer with modular amorphous core are presented.
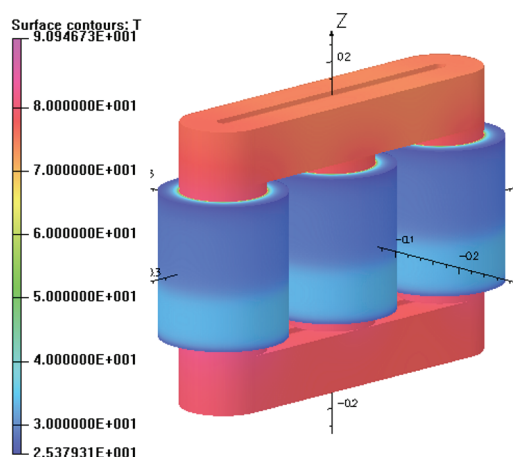

Fig. 4. The distribution of the calculated temperature, f_1 = 500 Hz

Due to supplying of the lower part of the transformer winding (N_1 = 20 turns) the temperature of the supplied coil is slightly higher than the upper one. For the frequency f_1 = 500 Hz, the temperature on the transformer body reaches 90°C. For the lower frequency (f_2 = 250 Hz) the maximal temperature is equal to 53°C. For the higher temperature, the radiation phenomena should be taken into account within the numerical calculations [7].
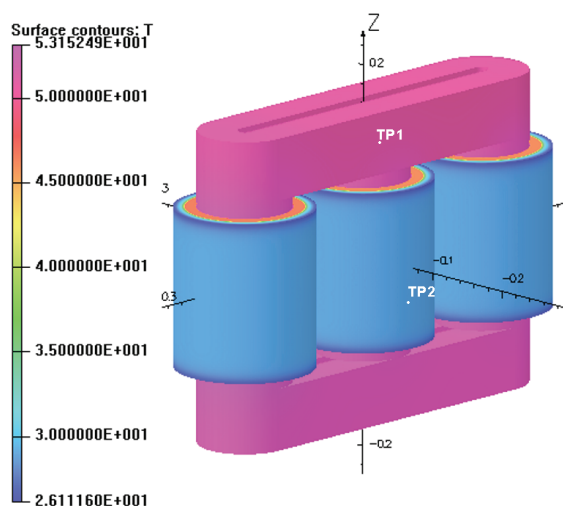

Fig. 5. The distribution of the calculated temperature, f_2 = 250 Hz

In Figures 6 and 7, the heating curves for both supplying frequencies are given. The presented curves concern the points TP1 and TP2 which are depicted in Figure 5. From the curves we can see that the analysed object reaches the static temperature after more than 5 hours of the transformer operation.
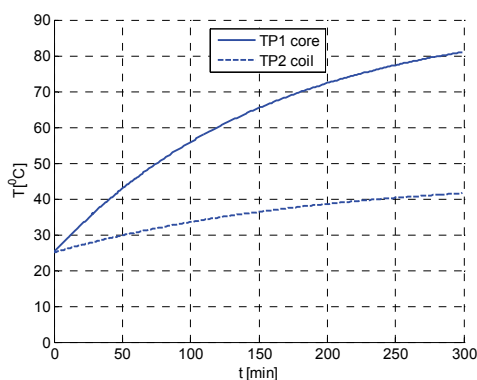

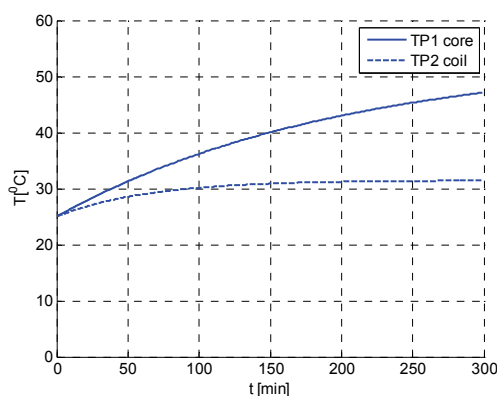Fig. 6. The calculated heating curves for TP1 and TP2, $f_1 = 500$ Hz

Fig. 7. The calculated heating curves for TP1 and TP2, $f_2 = 250$ Hz

The authors verified the calculation results by measurements with using thermal camera. Thus we made another calculations with frequency $f_2 = 250$ Hz sinusoidal supplying currents of the transformer. The values of ampere turns for A and C phases were equal to 105 A while the ampere turn was equal to 94 A for the phase B. For the assumed value of the equivalent conductivity $\sigma_{eq} = 500$ S/m, the calculated ($P_{Fe} = 130$ W) and measured ($P_{Fe} = 128$ W) total core losses were equal each to other The calculated histogram of the temperature is presented in Figure 8.

In Figure 9 is presented the histogram of the measured temperature distribution for the surface of the investigated transformer.

The differences between calculated and measured values result from neglecting in the thermal model the construction elements. Moreover, the assumed (for calculations) bottom insulation is not ideal and not extensive enough. Thus the maximum measured temperature of the core is lower than the calculated one. It amounts 46°C, while the calculated one is 52°C.
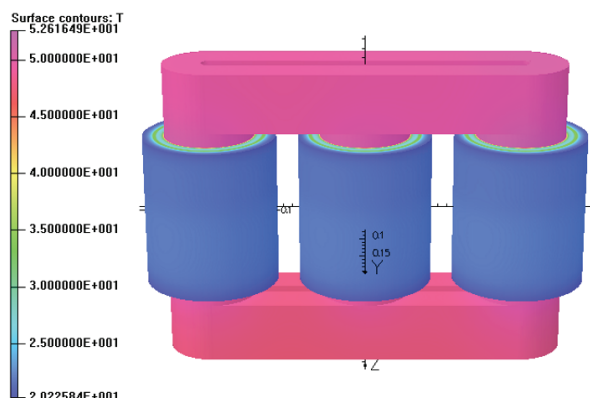

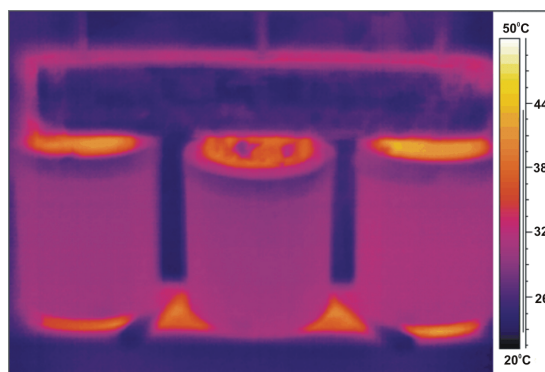Fig. 8. The calculated temperature on the analysed transformer for $f_2 = 250$ Hz

Fig. 9. The measured temperature on the surface of the analysed transformer (for $f_2 = 250$ Hz)

4. Conclusions

Due to the difficulties in the 3D numerical modeling of the field in transformer laminated amorphous core, the solid homogenized geometry of it should be implemented. To keep the same value of the eddy current losses of the core, the equivalent conductivity should be introduced. The losses value is the input datum for the thermal field analysis. For the temperature modeling the radiation phenomena should be taken into account.

Spatial distribution of the power losses inside the core enables calculating the so-called hot-spots in the transformer body. We have depicted the chosen points of the measured tem-

perature i.e. TP1 and TP2 at the core and winding bodies, respectively. For these points the heating curves (vs. time) have been obtained. Moreover, the histograms of the temperature at the transformer body have been performed. From the histograms of the calculated and measured temperatures, we noticed that the difference between maximal values of the core temperature amounts approximately 10%.

References

 [1] Binns K.J., Lawrenson P.J., Trowbridge C.W., *The Analytical and Numerical Solution of Electric and Magnetic Fields*. Chichester, U.K.Wiley (1992).
 [2] Lienhard IV J.H., Lienhard V J.H., *A heat transfer textbook.* 3rd ed., Phlogiston Press, Cambridge, Massachusetts, USA (2002).
 [3] OPERA Manager User Guide Version 13, Cobham Technical Services, Oxford, England (2009).
 [4] Sieradzki S., Rygal R., Soinski M., *Apparent Core Losses and Core Losses in Five-Limb Amorphous Transformer of 160 kVA.* IEEE Transactions on Magnetics, pp. 1189-1191 (1998).
 [5] Tomczuk B., *Numerical methods for field analysis of transformer systems.* Opole University of Technology Publishing, Opole (2007).
 [6] Tomczuk B., Koteras D., *Magnetic Flux Distribution in the Amorphous Modular Transformers.* Journal of Magnetism and Magnetic Materials, pp. 1611-1615 (2011)
 [7] Tomczuk B., Koteras D., Waindok A., *Electromagnetic and temperature 3d fields for the modular transformers heating under high frequency operation*. IEEE Transaction on Magnetics, pp. 700-704, (2014).
 [8] Tomczuk B., Waindok A., *Temperature distribution in multi domain construction of the permanent magnet linear actuator.* Archives of Electrical Engineering, pp. 417-424 (2013).
 [9] Wang J., Lin H., Huang Y., Sun X., *A new formulation of anisotropic equivalent conductivity in laminations*. IEEE Transactions on Magnetics, pp. 1378-1381 (2011).
[10] Zakrzewski K., *Power effect in magnetic lamination taking into account elliptical hysteresis approach*. ISEF'07, Prague, Czech Republic, no. 024 (2007).